Journal of Coastal Research	SI 50	211 - 215	ICS2007 (Proceedings)	Australia	ISSN 0749.0208

The Use of Video Systems to Measure Run-up on Beaches

S. A. Salmon†, K. R. Bryan† and G. Coco‡
†Dept. of Earth and Ocean Sciences University of Waikato, Hamilton, New Zealand
sas28@waikato.ac.nz
k.bryan@waikato.ac.nz
‡ National Institute of Water and Atmospheric Research, Hamilton, New Zealand
g.coco@niwa.co.nz

ABSTRACT

SALMON, S. A., BRYAN, K. R and COCO, G., 2007. The use of video systems to measure run-up on beaches. Journal of Coastal Research, SI 50 (Proceedings of the 9th International Coastal Symposium), 211 – 215. Gold Coast, Australia, ISSN 0749.0208

Wave run-up on beaches is a major driver of dune erosion and flooding during storm events on beaches. Using video imagery time-series collected over 2 field experiments, a new technique for measuring extreme run-up has been developed for use on natural beaches over a wide range of spatial and temporal scales. Waterline variations over 2 storm events were measured by collecting pixels from the video images along a cross-shore transect (timestack). The maximum swash excursions were digitized from the time-stacks, and rectified to provide a run-up time series with a duration of 20 minutes. In order to rectify run-up observations an estimate of the run-up elevation is needed. This was supplied using video measurements of the beachface morphology (e.g. beach slope). This was estimated by measuring the variation of the waterline over a tidal cycle from time-averaged video images taken during a storm event. This technique was tested against run-up measurements calculated using a standard empirical run-up equation and provides reliable estimates of run-up from video observations.

ADDITIONAL INDEX WORDS: *Foreshore morphology, Beachface, Swash excursions, Intertidal slope*

INTRODUCTION

Coastal dunes often provide the final defense line for coastal developments and properties against wave induced erosion. The amount of erosion depends on the water level height relative to the elevation of the fronting beach. This elevation is composed of the predicted astronomical tide level, storm surge associated with the inverse barometer effect and wind, wave set-up and wave run-up, (STOCKDON et al., 2006), with the latter being the most poorly understood. Wave run-up is responsible for causing much of the erosion of the beach and foredune (RUGGIERO et al., 2001). Moreover, if dune overtopping occurs this may lead to coastal flooding, resulting in loss of property and possibly lives. It is therefore important to accurately predict the magnitude and probability of occurrence of run-up.

One of the main impediments to making valid run-up predictions is the difficulty of obtaining observations of run-up over a wide range of storm wave conditions and beach types. In principle, run-up should vary with changes to the character of the incoming wave spectrum, but also with localized changes to surf-zone hydrodynamics, (such as rip current patterns), morphology, (such as foreshore slope), and sediment properties. Most *in situ* run-up experiments are conducted at a single location on the beach, and only over several weeks. Capturing a storm even over this time period is purely a matter of chance.

This paper presents a new technique for predicting the probability of dune erosion that is based on measuring run-up variation using sub-aerial video imagery of a beach. This is an extension on techniques developed by LIPPMANN and HOLMAN (1989) amongst many others. Here, run-up is defined as the maximum swash excursion and includes set-up as in STOCKDON et al. (2006). A comparison of run-up measurements derived from the video will be made with a well known empirical run-up predictor (i.e. HUNT, 1959)

FIELD SITE

Video imagery was collected on Tairua Beach on the Coromandel Peninsula, which is on the north east coast of the North Island of New Zealand. Tairua is an embayed beach that is constrained by headlands at either end of the beach. It is a tombolo, most frequently in an intermediate beach state (varying between 'longshore bar and trough' and 'transverse bar and rip') and is composed of medium-coarse sands. The beach has a northeast aspect and is therefore exposed to northerly and easterly swells (BOGLE et al., 2001), (Figure 1). Significant wave heights are low (<1.5 m), but can exceed 6 m during cyclone events. The tidal range is 1.2 m with little spring-neap variation.

METHODS

Run-up was measured from a 1 year database of video images of wave breaking patterns on Tairua Beach collected by the National Institute of Water and Atmospheric Research (NIWA). The video imaging system overlooking Tairua Beach is situated on the southern headland, Paku Hill, and is 70.5 m above chart datum. The system consists of a camera and computer which automatically collects images every daylight hour and offers a view which covers an area of dunes, beach and surfzone (BOGLE et al., 2001).

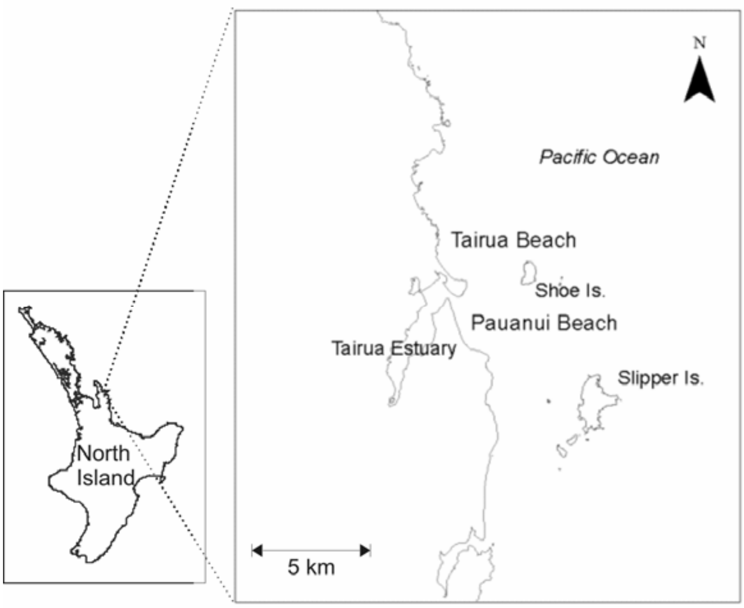

Figure 1. Map of New Zealand showing the location of the Tairua embayment in the Coromandel Peninsula

Wave and tidal information were extracted from the NIWA deepwater wave hindcast and tidal model output respectively. Atmospheric pressure data are measured at Whitianga airport approximately 10 kilometres to the north.

Video Images

Initial processing of the 760×570 images, performed automatically by a computer, produced three types of images 1) snapshots, which are taken at one moment in time 2) averages, which are a series of snapshots averaged over 20 minutes (Figure 2, bottom panel) and 3) time stacks, which are timeseries of pixels (usually covering a cross-shore transect on the beach face) collected over 20 minutes (Figure 2, top panel).

The averaged images from the video-image database were used to identify 2 storm events over the 1 year period. Averaging eliminates the variability in the run-up height of random individual waves, (BOGLE et al., 2001; BRYAN and SWALES, 2003; COCO et al., 2005), and allows a clear indication of the average height of the run-up and enables identification of the occurrence of erosive events. A storm event was defined as an event in which the waterline on the averaged images reached the toe of the dunes. The two worst storm events at the site were determined by simply choosing the images with the highest waterlines. The storms had significant wave heights, periods and durations of 5.3 m, 9.8 s and 68 hours for Storm 1 and 3.9 m, 10 s and 95 hours for Storm 2. Waves during both storm events approached from the northeast.

Run-up variations were measured by collecting pixels from the video images along a cross-shore transect in a time-stack (Figure 2, top panel). The maximum water line variation was manually digitized from the time-stacks, and rectified to provide run-up time series with a duration of 20 minutes.

Rectification

Known ground-control points were used to derive camera position and orientation (external camera parameters) which were then used to rectify the image, and thus change the format of the original images from oblique to plan form. These ground control points were surveyed using a Total Station. Prior to finding the external camera parameters, an internal camera calibration provided an estimate of the effective focal length, f, aspect ratio, optical centre and distortion coefficients. This was performed using software provided by HEIKKILA and SILVEN (1996). The combination of the internal and external camera calibration provided estimates of the camera position (X_0, Y_0, Z_0, where Z is the vertical dimension) and orientation (swing, s, tilt, τ, and azimuth, α) which were used to transform between image coordinates (x, y) into real-world coordinates (X,Y,Z). This transformation was accomplished using the colinearity equations

$$X=(Z-Z_0).Q+X_0 \tag{1}$$

$$Y=(Z-Z_0).P+Y_0 \tag{2}$$

where

$$Q=\frac{(m_{11}x+m_{21}y-m_{31}f)}{(m_{13}x+m_{23}y-m_{33}f)} \tag{3}$$

and

$$P=\frac{(m_{12}x+m_{22}y-m_{32}f)}{(m_{13}x+m_{23}-m_{33}f)} \tag{4}$$

where m_{ij} are the elements of the 3×3 matrix M

$$M=\begin{pmatrix}\cos(\alpha) & \sin(\alpha) & 0\\ \sin(\alpha) & \cos(\alpha) & 0\\ 0 & 0 & 1\end{pmatrix}\begin{pmatrix}1 & 0 & 0\\ 0 & \cos(\tau) & -\sin(\tau)\\ 0 & \sin(\tau) & \cos(\tau)\end{pmatrix}\begin{pmatrix}-\cos(s) & -\sin(s) & 0\\ -\sin(s) & \cos(s) & 0\\ 0 & 0 & 1\end{pmatrix}$$

In order to use the colinearity equations to transform between x, y and X, Y a known value of Z must be supplied.

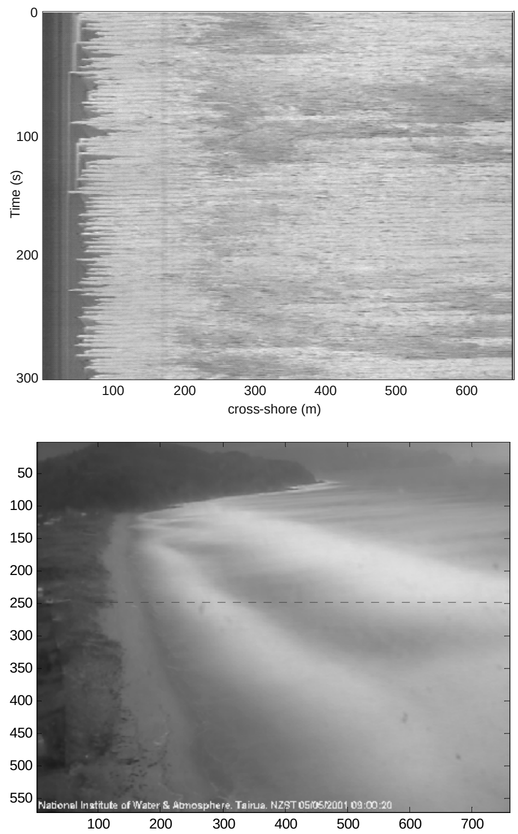

Figure 2. Top panel: Timestack. Bottom panel: Averaged video image of Tairua Beach showing position at which timestacks are taken. The coordinates of the line are from (95, 248) to (760, 248).

Run-up Measurement

In the case of estimating run-up from video, a prior assumption of the value of Z is not made. Ideally, information supplied by the camera would be used to infer Z as well as X and Y. It is possible to collect information on the foreshore slope by tracking the edge of the waterline in the time-averaged images as the tide ranges from low to high (or vice versa). If the beach face is linear, this information can be used to define foreshore slope, a, and intercept, b, where

$$Z = aX + b \tag{5}$$

which provides an estimate of the Z value needed for rectification.

In practice, time-averaged video images over a complete tidal cycle during the selected storm event were used to define the foreshore slope. The waterline for each image was detected using a computer routine which searched the image for gradients in the ratio of red to green light. A subjectively chosen threshold of 1 appeared to correspond well to the location of the shoreline (SMITH and BRYAN, in press) (Figure 3). Comparison with beach surveys at Tairua have shown that this provides a fairly accurate estimate of foreshore slope, and that Tairua Beach does have a intertidal region with a slope that does not vary appreciably in the cross-shore as necessitated by the method. Note that the slope does vary in the alongshore direction, so a new estimate of slope is needed if the location where the timestack is collected is changed.

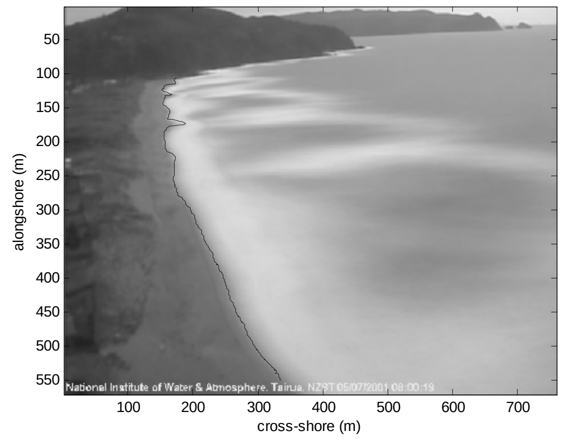

Figure 3. Video image showing a digitised shoreline

Combining equations (1) (2) and (5) gives

$$X = \frac{Qb - QZ_0 + X_0}{(1 - aQ)} \tag{6}$$

and

$$Y = \frac{Pb - PZ_0 + Y_0}{(1 - aP)}. \tag{7}$$

Wave Set-up and the Inverse Barometer Effect

In order to obtain accurate results, the Z used in determining slope and intercept in equation (5) should also include the influence of set-up and the inverse barometer effect. Set-up causes an elevated water level inside the surf zone. In the absence of measurements of set-up and detailed surf-zone wave information, we use BOWEN *et al.* (1968) to calculate wave set-up

$$\eta_{set-up} = \frac{3}{8}\gamma^2 \frac{(h_b + \eta_{tide})}{\left(1 + \frac{3}{8}\gamma^2\right)^2} \tag{8}$$

where

$$h_b = \frac{H_{rms}}{\gamma} \tag{9}$$

We have used a γ of 0.4 which is roughly consistent with observations (e.g. RUESSINK et al., 2003).

The inverse barometer effect was included in the water level as a 0.1 m sea level rise for every 10 hPa drop in atmospheric pressure that occurred during the passage of the low-pressure systems associated with each storm event.

RESULTS

During both storm events, the main contributors to the mean water level at high tide were the tide and set-up. The high tide water level for storm 1 was 1.90 m above chart datum (mean sea level is 1 m above chart datum), which included a 0.50 m contribution from set-up. During storm event 2, the water levels averaged 1.93 m above chart datum with a 0.48 m wave set-up contribution. The inverse barometer effect was minimal because the storm systems were not associated with a significant local atmospheric pressure drop, and consisted of a water level rise of 6 cm for both storms.

The average water lines, digitized from the images and rectified, had a consistent cross-shore range along the beach (Figure 4, top panel), indicating the foreshore slope was similar along the beach, varying somewhat with the cuspate beachface morphology. The calculated foreshore slopes were 0.075 and 0.083 for storms 1 and 2 respectively. Although there was some variability caused by digitization and shoreline recognition errors, the regression was still good (r^2 = 0.638 for storm 1 and r^2 = 0.685 for storm 2) (Figure 4, bottom panel).

Calculated high tide run-up values averaged 0.72 m and 0.41 m (maxima 1.4 and 0.9 m and minima -0.12 and -0.42 m) for storms 1 and 2 respectively. Low tide run-up levels averaged 0.44 m and 0.34 m (maxima levels of 1.6 m and 1.73 m and minima -0.72 m and -1.15 m) for storms 1 and 2 respectively (Figure 5). Distributions were very slightly non-gaussian (which was also noted in STOCKDON et al., 2006) although a greater number of run-up events need to be sampled to confirm this.

DISCUSSION

The ranges of run-up found in the study appear to be realistic measuring between -0.4–1.4 m during high tide and -0.5–1.4 m during low tide. This demonstrates that it is indeed possible to derive estimates of run-up using remote video techniques. This will allow the exciting possibility of continuous run-up estimates during storms, along with the ability to measure alongshore variations to run-up associated with alongshore morphology changes both in the beachface and in the offshore bars.

In order to determine whether the run-up values observed here are realistic, comparison can be made by parameterizations of run-up. Hunt (1959) is often used (see for example STOCKDON et al., 2006) where

$$R = K \xi_{\infty} H_{\infty} \tag{10}$$

where K is equal to 0.45 and ξ_{∞} is the Iribarren number equal to

$$\xi_{\infty} = \frac{\tan\beta}{\sqrt{\dfrac{H_{\infty}}{L_{\infty}}}} \tag{11}$$

where H_{∞}, β, L_{∞} are the deep water wave height, beach slope and the deepwater wavelength respectively.

Comparisons between the Hunt equation and video image run-up results were made to test the run-up measurement technique used in this study. The Hunt equation produces run-up measurements of 1.46 m and 0.96 m for storms 1 and 2 at high tide and Iribarren numbers of 0.66 and 0.55 respectively. The same run-up patterns for the storms are achieved in that the results using the Hunt equation show that run-up was smaller in storm 2. Moreover the difference between the observed run-up for the two storms is 0.4, which is comparable to the differences predicted by Hunt (1959).

The absolute value of the video run-up measurements however did not compare well to the Hunt equation. Furthur investigation shows that the absolute value of the run-up measurements from video depend upon correctly identifying the cross-shore location of the average water line, which is used in equation (5). The red to green ratio appears to find a water line that is somewhat landward of the actual water line which translates as an intercept in equation (5) that is too small. Correcting this to a more seaward value makes the run-up measurements from video much more comparable to Hunt (1959). Some ground truthing is clearly

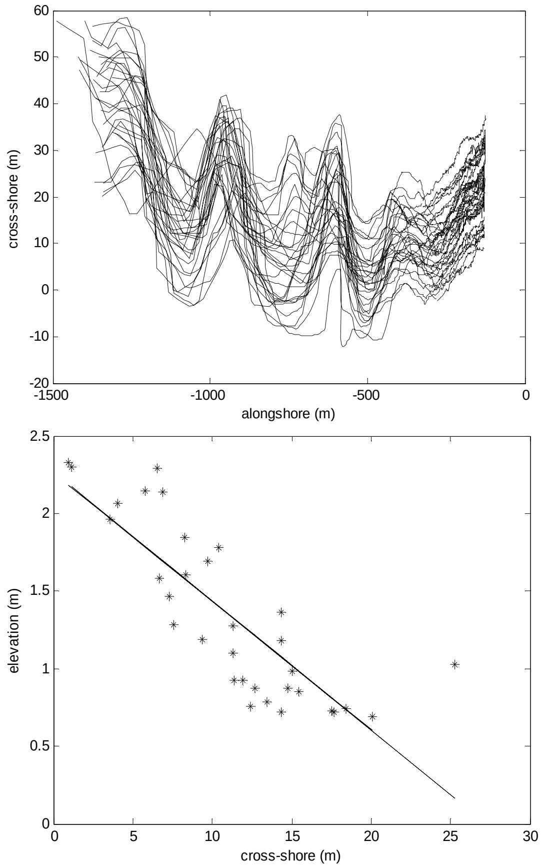

Figure 4. Top panel: full tidal cycle of rectified and rotated waterlines. Bottom panel: waterline heights versus cross-shore location at the longshore location at which the timestack was collected (pixel coordinate y = 248).

needed to ascertain the location of the actual water line relative to the water line derived from video.

The other main sources of error associated with this technique include inaccuracies in the waterline finding routines. Slight variations in the colour of the beach sand relative to the water caused by lighting and breaking variations can cause variations, along with blurring in the image caused by fog and rain on the lens. There are also errors associated with the inaccuracies in Z and surveying. These combined errors have been shown to be less than 15 cm (AARNINKHOF et al., 2003), however this will depend on the geometry of the camera, and nature of the shoreline finding algorithm. Our surveying errors are very small (< 2 cm).

The next step is to validate the technique used in this paper over a wider range of storm conditions and beach face slopes, and also to compare the technique to modeled run-up estimates. Measuring the alongshore variation of run-up and the controls on this (which can make the results vary by up to 41% according to STOCKDON et al., 2006) is also a logical next step.

CONCLUSION

A new technique for measuring run-up using remote video imagery of the beach has been outlined and tested. Preliminary results indicate that the technique can give realistic run-up measurements, and can provide measurements of run-up for a wide range of time scales, all along a beach and during storm events when the hydrodynamic conditions may be too dangerous

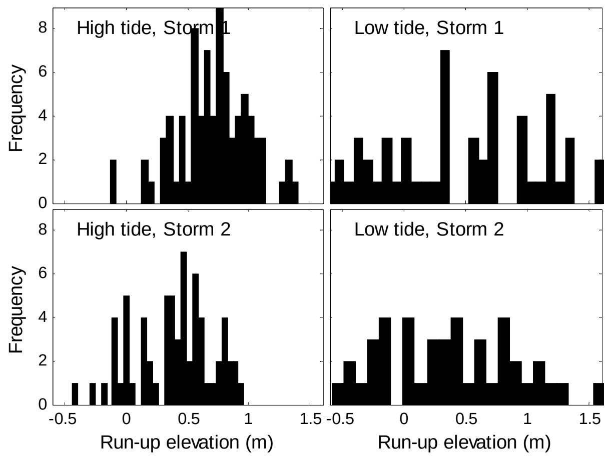

Figure 5. Histograms showing run-up (swash excursion and set-up) statistics of both storm events at high and low tides. The zero level is the level of the tide.

to collect field measurements. The absolute value of the video run-up measurements however did not compare well to the standard empirical run-up formula we tested and furthur investigation needs to be carried out in order to ensure the cross-shore location is correctly identified.

ACKNOWLEDGEMENTS

SAS was funded by Te Tipu Pūtaiao Masters Fellowship, The Broad Memorial Fund, and the University of Waikato. GC is funded by the (New Zealand) Foundation for Research, Science and Technology (contracts C01X0401).

LITERATURE CITED

AARNINKHOF, S.G.J.; TURNER, I.L.; DRONKERS, T.D.T.; CALJOUW, M., and NIPIUS, L., 2003. A video-based technique for mapping intertidal beach bathymetry, *Coastal Engineering*, 49, 275–289.

BOGLE, J.A.; BRYAN, K.R.; BLACK, K.P.; HUME, T.M., and HEALY, T.R., 2001. Video Observations of Rip Formation and Evolution*, Journal of Coastal Research,* Special Issue, 34, 117–127.

BOWEN, A.J.; INMAN, D.L., and SIMMONS, V.P., 1968. Wave 'set-down' and 'set-up'. *Journal of Geophysical Research*, 73(8), 2569–2577.

BRYAN, K.R., and SWALES, A., 2003. Inferring bar position from video imagery of breaking waves at Tairua Beach, New Zealand. *Proceedings of Coasts and Ports*, Auckland, New Zealand, paper #20.

COCO, G.; BRYAN, K.R.; GREEN, M.O.; RUESSINK, B.G.; TURNER, I.L. and VAN ENCKEVORT, I.M.J., 2005. Video observations of shoreline and sandbar coupled dynamics. *Proceedings of Coasts and Ports*, Adelaide, Australia, pp. 471–476.

HUNT, I.A., 1959. Design of seawalls and breakwaters. *Journal of Waterways and Harbours Division*, ASCE 85 (WW3), 123–152.

HEIKKILA, J. and SILVEN, O., 1996. Calibration procedure for short focal length off-the-shelf CCD cameras. In: *Proc of The 13th International Conference on Pattern Recognition.* Vienna, Austria: pp. 166–170.

LIPPMANN, T. C. and HOLMAN, R. A., 1989. Quantification of sand bar morphology: A video technique based on wave dissipation. *Journal of Geophysical Research*, 94(C1), 995–1011.

RUESSINK, B. G.; WALSTRA, D. J. R.; and SOUTHGATE, H. N. 2003. Calibration and verification of a parametric wave model on barred beaches, *Coastal Engineering*, 48, 139–149.

RUGGIERO, P.; KOMAR, P.D.; MCDOUGAL, W.G.; MARRA, J.J., AND BEACH, R.A., 2001. Wave run-up, extreme water levels and the erosion of properties backing beaches. *Journal of Coastal Research*, 17(2), 407–419.

SMITH, R. K. and BRYAN, K. R., Monitoring beachface volume using a combination of intermittent profiling and video imagery. *Journal of Coastal Research*, in press.

STOCKDON, H.F., HOLMAN, R.A., HOWD, P.A. and SALLENGER JR., A.H., 2006. Empirical parameterization of setup, swash, and runup, *Coastal Engineering*, 53, 573-588